

# An Efficient Generator of Synthetic Turbulence at RANS–LES Interface in Embedded LES of Wall-Bounded and Free Shear Flows

Dmitry Adamian and Andrey Travin

**Abstract** A new simple method is presented for generating velocity fluctuations at the inflow of LES domain in Embedded LES. The method employs only RANS turbulence statistics and is shown to be rather accurate in both canonical shear flows (plane channel, zero pressure gradient boundary layer, and plane mixing layer) and in a wall-mounted hump flow with pressure-induced separation and reattachment.

## 1 Introduction

Hybrid RANS–LES approaches to turbulence representation are now considered as the only currently manageable alternative to the pure RANS of complex turbulent flows at high Reynolds numbers. One of the most flexible approaches of this type is the so-called Embedded LES (ELES), which assumes using LES only in a restricted arbitrary specified flow region(s) where pure RANS is incapable or turbulent content of the flow is for some reason essential, whereas the rest of the flow is treated with RANS. A key prerequisite of these approaches in the case when LES region is located downstream of RANS area is a robust way to produce realistic turbulent content at the RANS–LES interface. A number of methods aimed at resolving this challenging problem have been proposed, including the use of external databases from LES or DNS of simple flows (e.g., the developed channel flow), different recycling/rescaling procedures, and “synthetic turbulence” generators. All these methods have their pros and cons. For instance, the recycling methods are capable of creating a natural inflow turbulence but are applicable only in the nearly equilibrium flow regions. The synthetic methods are, in principle, more flexible. However some of them require too detailed knowledge of turbulent statistics (length-scales, time- and space-correlation functions, etc.) which could not be provided by RANS models used upstream of the RANS–LES interface while using the other ones results in realistic turbulence structures being established too slow, thus causing significant degradation of the whole solution.

---

D. Adamian (✉)

St. Petersburg State Polytechnic University, St. Petersburg 195257, Russia  
e-mail: dmitry.adamian@gmail.com

In the present work a new simple ad hoc algorithm is proposed for generation of “synthetic turbulence” (velocity fluctuations) at the inflow of LES domain which employs only the turbulent quantities involved in the conventional two-equation RANS models and, at the same time, ensures fairly rapid transition to physically realistic turbulence. The algorithm employs ideas of Bechara et al. [1] who proposed a harmonic generator of turbulence for stochastic noise modeling and some elements of other available turbulence generators. However, unlike these methods, it is capable of plausible representation of anisotropy of the vortical structures, which is an essential feature of the near-wall turbulence.

## 2 Formulation

Let  $\mathbf{U}(\mathbf{r})$  be the mean velocity at RANS–LES interface known from the RANS solution. Then the velocity field  $\mathbf{u}(\mathbf{r}, t)$  imposed as the inflow boundary condition for LES at this interface is defined as follows:

$$\mathbf{u}(\mathbf{r}, t) = \mathbf{U}(\mathbf{r}) + \mathbf{u}'(\mathbf{r}, t), \quad (1)$$

where  $\mathbf{u}'(\mathbf{r}, t)$  is the field of velocity fluctuations (“synthetic turbulence”).

Similar to other methods of the same type (e.g., [4]),  $\mathbf{u}'(\mathbf{r}, t)$  is defined so that the corresponding second moment tensor  $\langle u'_i u'_j \rangle$  is equal to the Reynolds stress tensor  $\mathbf{R}$  known from the RANS solution. This is reached by using Cholesky decomposition of the Reynolds stress tensor  $\mathbf{R} = \mathbf{A}^T \mathbf{A}$ . Then the synthetic velocity fluctuations in (1) can be defined via elements of the tensor  $\mathbf{A}$  as  $u'_i(\mathbf{r}, t) = a_{ij}(\mathbf{r}) v'_j(\mathbf{r}, t)$ , where  $\mathbf{v}'_j(\mathbf{r}, t)$  is the auxiliary field of the velocity fluctuations satisfying  $\langle v'_j \rangle = 0$  and  $\langle v'_i v'_j \rangle = \delta_{ij}$ . Thus the problem of definition of  $\mathbf{u}'(\mathbf{r}, t)$  in (1) reduces to definition of the  $\mathbf{v}'(\mathbf{r}, t)$  field. In the present work, this field is prescribed in the form of superposition of weighted Fourier modes:

$$\mathbf{v}'(\mathbf{r}, t) = \sqrt{6} \sum_{n=1}^N \sqrt{q^n} \left[ \boldsymbol{\sigma}^n \cos \left( k^n \mathbf{d}^n \cdot \mathbf{r} + \phi^n + s^n \frac{t}{\tau} \right) \right] \quad (2)$$

Here:  $N$  is the number of modes, which is defined during the computations (see below);  $q^n$  is the normalized amplitude of the  $n$ -th mode defined by the local energy spectrum;  $k^n$  is the wave number of the  $n$ -th mode;  $\mathbf{d}^n$  is the random wave vector direction uniformly distributed over unit sphere;  $\boldsymbol{\sigma}^n$  is the unit vector normal to  $\mathbf{d}^n$ , and the angle defining its direction in the plane is a random number uniformly distributed in the interval  $[0, 2\pi)$ ;  $\phi^n$  is the phase of the  $n$ -th mode, which is also a random number uniformly distributed in the interval  $[0, 2\pi)$ ;  $s^n$  is the non-dimensional frequency of the  $n$ -th mode with Gaussian distribution and the mean value and standard deviation equal to  $2\pi$ ;  $\tau$  is the global time-scale.

Normalized amplitudes of the modes in (2)

$$q^n = E(k^n)\Delta k^n / \sum_{n=1}^N E(k^n)\Delta k^n, \quad \sum_{n=1}^N q^n = 1 \quad (3)$$

are defined with the use of a modified von Karman spectrum (see Fig. 1):

$$E(k) = (k/k_e)^4 \left[ 1 + 2.4 (k/k_e)^2 \right]^{-17/6} f_\eta f_{cut} \quad (4)$$

Here  $f_{cut}$  and  $f_\eta$  are empiric functions. The former provides damping of the spectrum in the vicinity of wave number corresponding to the Kolmogorov length-scale (it is designed based on the classic experiments of Comte-Bellot and Corsinn [2]) and the latter damps the spectrum for wave numbers larger than the Nyquist one,  $k_{cut} = 2\pi/l_{cut}$ . The functions read as  $f_\eta = \exp[-(12k/k_{eta})^2]$  and  $f_{cut} = \exp\{-[4 \max(k - 0.9k_{cut}, 0)]^3 / k_{cut}\}$ , where  $k_\eta = 2\pi / (\nu^3/\varepsilon)^{1/4}$  ( $\nu$  is the molecular viscosity,  $\varepsilon$  is the turbulence dissipation rate), and the wave length  $l_{cut}$  is defined as  $l_{cut} = 2 \min\{[\max(h_y, h_z, 0.3h_{max}) + 0.1d_w], h_{max}\}$  with  $h_y$  and  $h_z$  being the local grid steps in the LES inflow section,  $h_{max} = \max(h_x, h_y, h_z)$ , and  $d_w$  is the distance to the wall.

Finally, the wave number  $k_e$  in (4) corresponding to the maximum of the spectrum  $E(k)$  is defined by wave length of the most energy-containing modes,  $l_e$ , of the synthetic velocity fluctuations or, in other words, by size of the most energy-containing eddies:  $k_e = 2\pi/l_e$ . Note that a proper choice of  $l_e$  is of crucial importance for getting the velocity field rapidly evolving to the physically realistic one. In present work this length-scale is defined as follows:

$$l_e = \min(2d_w, C_l l_t) \quad (5)$$

where  $C_l = 3$  is an empirical constant and  $l_t$  is the length-scale of the turbulence model used in RANS region (for instance,  $l_t = k_t^{1/2} / (C_\mu \omega_t)$  in the case if this is  $k - \omega$  model).

In the near-wall part of the flow (5) returns  $l_e$  equal to the doubled distance to the wall, whereas in the outer part of the boundary layer it reduces to the RANS length-sale. Examples of  $l_e(d_w)$  distributions in the canonic turbulent shear flows computed with the use of  $k - \omega$  SST model [5] are presented in Fig. 2.

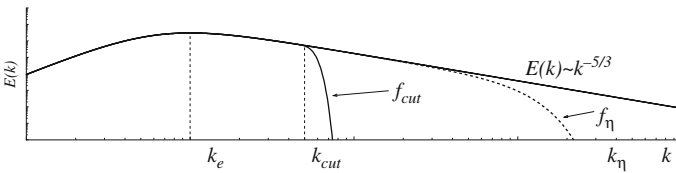
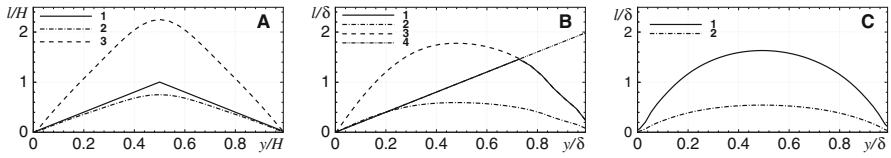


Fig. 1 Energy spectrum of the synthetic velocity fluctuation field



**Fig. 2** Distribution of the length-scales involved in (5) in a plane channel (a), ZPGBL (b), and plane free shear layer (c). 1 –  $l_e$ , 2 –  $l_t$ , 3 –  $C_l l_t$ , 4 –  $2d_w$

A set of the wave numbers used in the turbulence generator (2) is common for the whole RANS–LES interface and forms geometric series  $k^n = k^{\min} \cdot (1 + \alpha)^{n-1}$ ,  $n = 1 \div N$ ,  $\alpha = 0.01 \div 0.05$  (here  $k^{\min} = \beta k_e^{\min}$  is the minimum wave number,  $\beta = 0.5$ , and  $k_e^{\min}$  is the wave number corresponding to the maximum value of  $l_e$ :  $k_e^{\min} = 2\pi/l_e^{\max}$ ,  $l_e^{\max} = \max\{l_e(\mathbf{r})\}$ ). The value of  $N$ , i.e., the number of modes used in (2) is the maximum integer, for which  $k^N$  satisfies the inequality  $k^N \leq k_{\max} = 1.5 \max\{k_{cut}(\mathbf{r})\}$ .

To finalize the formulation, we have to specify the time-scale  $\tau$  in (2). It is defined via the quantity  $l_e^{\max}$  and a macro-scale of the velocity in the interface section (e.g., the maximum or bulk velocity):  $\tau = C_\tau l_e^{\max}/U$ ,  $C_\tau$  is the empiric constant. Note that exactly such global definition of the time-scale, coupled with the local scale of the energy-containing eddies  $l_e$  (5) results in forming of physically realistic (elongated in the streamwise direction) eddies in the inner part and nearly isotropic eddies in the outer part of the boundary layer.

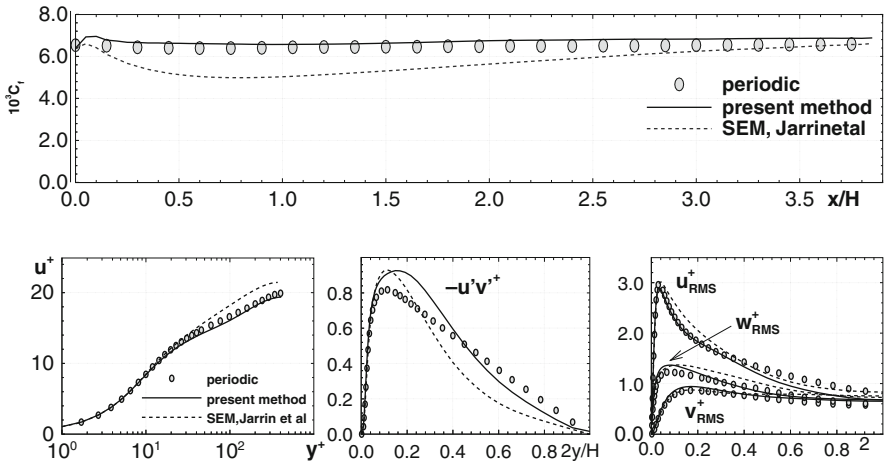


**Fig. 3** Skin-friction distributions and mean velocity and Reynolds stresses profiles in the plane channel at  $Re_\tau = 400$  predicted by hybrid algebraic WMLES model [6] with different inflow conditions (results with streamwise-periodic BCs are considered as a benchmark)

### 3 Results

The method outlined above has been applied to LES of three canonical shear flows: a channel flow at  $Re_\tau = 400$ , zero pressure gradient boundary layer (ZPGBL), and plane free shear layer. In all the cases the simulations were performed with the use of the algebraic hybrid WMLES model [6]. Results of the simulations shown in Figs. 3, 4 and 5 suggest that the inflow turbulent content created by the proposed method indeed ensures a rapid formation of realistic turbulent structures farther downstream: the length of relaxation from the inflow section to a mature LES solution turns out to be tangibly shorter than that with Synthetic Eddy Method (SEM) [4] currently considered as one of the best synthetic turbulence generators (see Fig. 3) and comparable to that with the recycling method [7] (see Fig. 4).

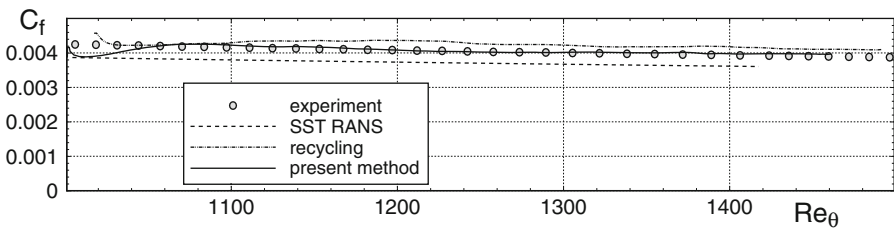


Fig. 4 Comparison of skin-friction distributions in ZPGBL predicted with the use of different inflow conditions

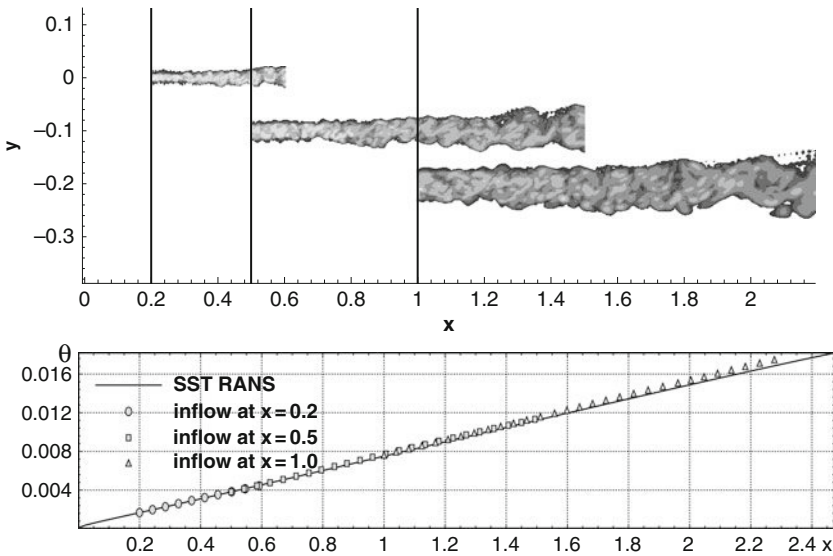
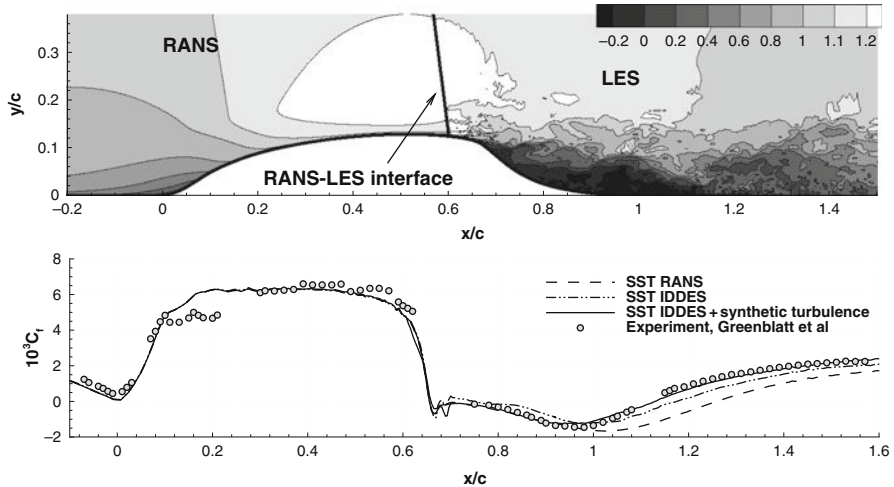


Fig. 5 Snapshots of vorticity contours and downstream evolution of the momentum thickness of the free shear layer from ELES with different locations of the RANS–LES interface



**Fig. 6** Snapshot of streamwise velocity from Embedded IDDES and skin-friction distributions predicted with the use of different approaches for the wall-mounted hump flow [3]

The proposed method combined with the  $k - \omega$  SST based Embedded IDDES [6] has also been applied to the flow past a wall mounted hump at  $Re = 936000$  studied experimentally in [3]. Results of the simulation shown on Fig. 6 visibly demonstrate a significant improvement of the agreement with the experiment in the case of Embedded IDDES with the proposed synthetic velocity fluctuations at the RANS-IDDES interface compared to both RANS and IDDES in the whole domain.

**Acknowledgements** This work was funded by the EU ATAAC (ACP8-GA-2009-233710) project, by Boeing Commercial Airplanes and, partially, by the Russian Basic Research Foundation (grant No. 09-08-00126).

## References

1. Bechara, W., Bailly, C., Lafon, P., Candel, S.M.: Stochastic approach to noise modeling for free turbulent flows. *AIAA J.* **32**, 455–463 (1994)
2. Comte-Bellot, G., Corrsin, S.: Simple Eulerian time correlation of full- and narrow-band velocity signals in grid-generated, “isotropic” turbulence. *J. Fluid Mech.* **48**, 273–337 (1971)
3. Greenblatt, D., Paschal, K., Yao, C.-S., Harris, J.: A separation control CFD validation test case part 2. Zero Efflux oscillatory blowing. 43rd AIAA Aerospace Sciences Meeting and Exhibit, Reno, NV, AIAA Paper 2005-0485 (2005)
4. Jarrin, N., Benhamadouche, S., Laurence, D., Prosser, R.: A synthetic-eddy-method for generating inflow conditions for large-eddy simulations. *Int. J. Heat Fluid Flow.* **27**, 585–593 (2006)
5. Menter, F.R.: Two-equation eddy-viscosity turbulence models for engineering applications. *AIAA J.* **32**, 1598–1605 (1994)
6. Shur, M., Spalart, P.R., Strelets, M., Travin, A.: A hybrid RANS-LES approach with delayed-DES and wall-modelled LES capabilities. *Int. J. Heat Fluid Flow.* **29**, 1638–1649 (2008)
7. Spalart, P.R., Strelets, M., Travin, A.: Direct numerical simulation of large-eddy-break-up devices in a boundary layer. *Int. J. Heat Fluid Flow.* **27**, 902–910 (2006)